From Eye to Insight

Application Note

EXPLORATION OF 3D TISSUE MICROENVIRONMENT USING AI-POWERED MULTIPLEXED IMAGE ANALYSIS

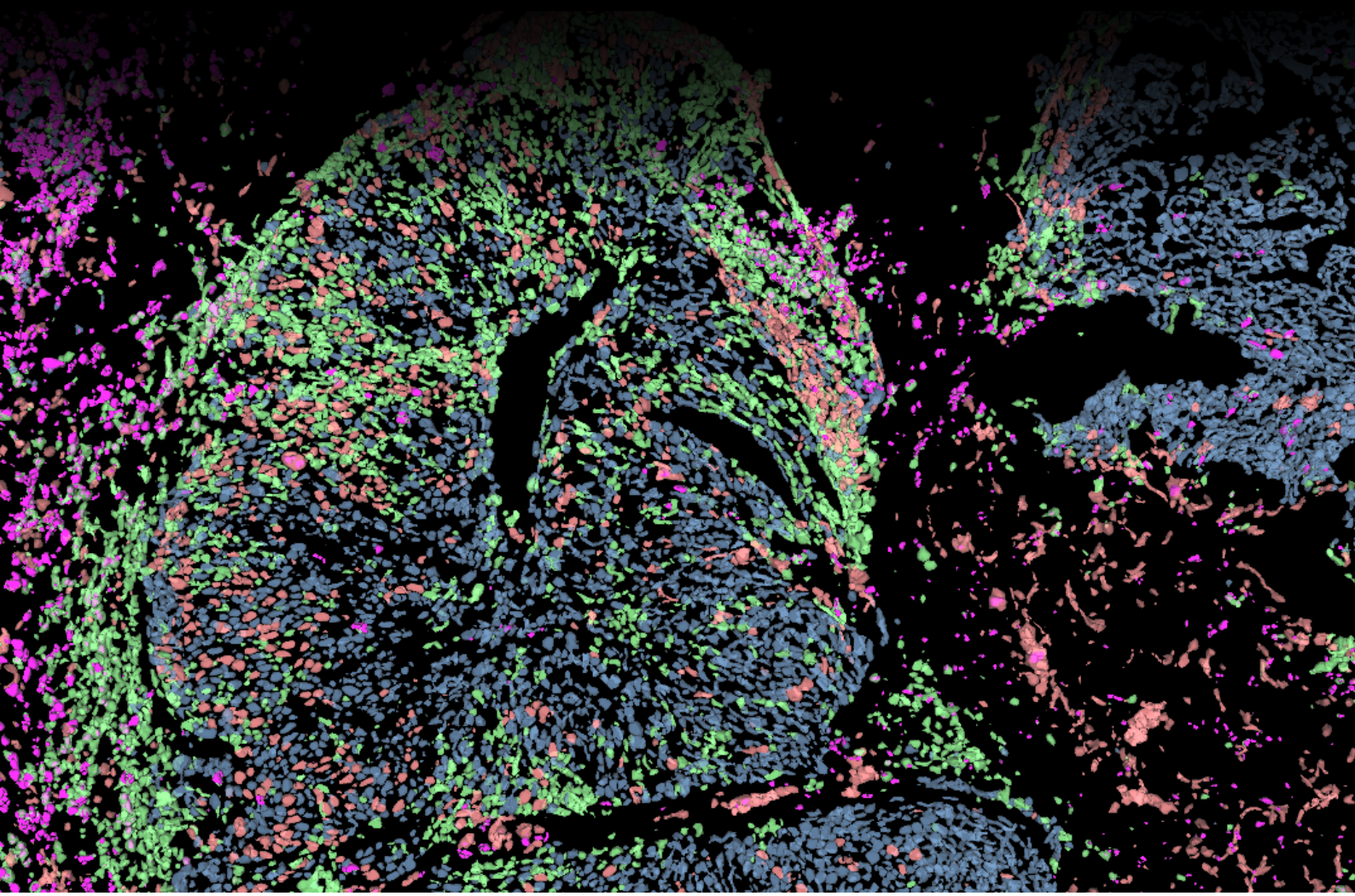

Authors

Hoyin Lai, Tatjana Straka, Ph.D., Frank Hecht, Vasundhara Agrawal, Ph.D., Michael Smith, Ph.D., Won Yung Choi, Ph.D.

Introduction

Tumor formation during oncogenesis often followed by the formation of a specialized niche in the host in response to stimuli produced by cancer cells. The resulting tumor microenvironment is a complex system in which cancer cells interface with host tissue, organs, and the immune system[1]. These interactions influence the tumor progression and the efficacy of cancer therapies. Owing to the complexity of the tumor microenvironment, novel technologies and techniques have been leveraged to accurately identify the cells and biological processes at play in these complex tumor microenvironments. Spatial biology techniques that combine high-throughput information about biological analytes like RNA and protein with positional information offer the potential for significant advances in understanding cancer biology within the tumor microenvironment. In the field of microscopy, innovations in labeling techniques have allowed for a higher number of protein markers to be targeted and visualized through antibody-based techniques. However, capturing high-resolution images of these markers presents significant technical challenges, especially in 3D with higher physiological relevance. The resulting data often comprises tens of thousands of cells and multiple fluorescent channels. This wealth of information is key to understanding the biological processes found in physiological conditions, yet they can pose significant technical and computing challenges.

Here, we present a detailed 3D spatial analysis of eight immuno-oncology relevant biomarkers in lung cancer tissue. We acquired 3D images on a STELLARIS confocal platform equipped with the SpectraPlex functionality[2] to seamlessly capture the rich multiplexed information in one go and with 3D spatial context. To extract the spatial insights, we defined a workflow to segment, phenotype, and perform spatial relational analysis on cells within the tissue using the Aivia analysis software. We gain insight into cellular identities within the tumor microenvironment, as well as detailed information about immune cell positioning in this cancer sample.

Methods

To explore the tumor microenvironment, we made use of a lung cancer tissue section sourced from Discovery Life Sciences Biomarker Services (Kassel, Germany) as a representative example. The sample was then stained sequentially with 8 antibodies targeting Ki67, FoxP3, PD-L1, CD4, CD68, CD3, CD8, panCK, each conjugated with an Opal™ fluorophore, and DAPI as a nuclear counterstain (Table 1).

Table 1. Biomarker Panel

Marker	Cellular Location	Dye	Excitation (Max, nm)	Emission (Max, nm)	Marker Role
Ki67	Nucleus	Opal 480	450	500	Cellular Proliferation
FoxP3	Nucleus	Opal 520	494	525	Regulatory T Cell (Treg) marker
PD-L1	Membrane	Opal 540	523	536	Immune checkpoint
CD4	Membrane	Opal 570	550	570	T helper marker
CD68	Membrane	Opal 620	588	616	Monocyte/macrophage marker
CD3	Membrane	Opal 650	627	650	T cell marker
CD8	Membrane	Opal 690	676	694	T killer marker
PanCK	Membrane	Opal 780	750	770	Epithelial/tumor marker
DNA	Nucleus	DAPI	359	461	Nuclear counterstain

We then carried out the acquisition all labeled markers present in one round of imaging. To define the experiment, the targets and dyes were combined into markers in the SpectraPlex “Virtual Fridge”. From this panel, SpectraPlex presents optimized acquisition settings, tuning excitation and detection to maximize signal-to-noise ratio after unmixing and minimize crosstalk. The settings were then used to acquire data to generate an unmixing matrix directly from the sample stained with the full panel[3].

SpectraPlex reduces study design time and reduces time-to-result for complex 3D sample types and multiplexed imaging. SpectraPlex can be used to acquire multiplexed datasets of 15+ biomarkers and is also well suited to smaller panels and offers significant time savings and ease-of-use compared to manual creation of imaging settings and unmixing parameters.

Detecting cells in multiplexed image volumes with AI

After image acquisition, we performed an end-to-end 3D spatial analysis of the samples using the AI-powered analysis tools in Aivia. In general, multiplexed analysis, whether in 2 or 3D, follows a standard process. Cells are first recognized in software and segmented to make them tractable to downstream analysis. Then, based on expression levels of biomarkers within those defined and segmented cellular territories, phenotyping of the cells can be undertaken. This can be approached in a supervised fashion, using a user's expert knowledge to define which biomarker positivities correspond to which biological phenotypes, but can also be performed in an unsupervised manner using clustering algorithms. More detailed spatial relational analysis can then be undertaken to determine whether the physical positions of different cell types in the sample vary according to phenotype.

Detection of individual cells

Detection and segmentation of individual cells in whole image volumes is the first step toward quantitative spatial analysis and biological insight generation. Accurate segmentation of individual cells in a tissue section presents a particular challenge due to the potential spatial overlap between cells across a 3D image stack. Aivia's machine learning-based Pixel Classifier can enhance the membrane signal to improve spatial separation between individual cells. By painting a few sections of the cell membrane, Aivia improves the signal of the labeled membranes (Figure 1). The 3D Multiplexed Cell Detection recipe in Aivia leverages a modified Cellpose algorithm[4] to detect cells with different morphologies in the tissue accurately. We applied the segmentation recipe to the epithelial cells (PanCK), T-cells (CD3, CD4, CD8), and B-cells (CD68) separately, to improve the segmentation accuracy and predictive power of the downstream cell classifier. In total, 21,244 epithelial cells, 5,724 T-cells, and 195 B-cells were segmented, with an average volume of 160.65 μm^3, 102.20 μm^3, and 123.36 μm^3 respectively.

Classification and phenotyping of known and unknown cell populations

Examining the cell phenotypes that are present in the image represents the next step in spatial analysis of the tissue microenvironment. Understanding the types of cells that are present, their abundance, and their spatial distribution in the tissue could infer the state of the tissue. Using Aivia's Classifier tool, it is possible to separate the cells by providing a few examples of each phenotype. As the epithelial cells and B-Cells are separately segmented and classified, we applied the Automatic Classifier to the T Cells group and identified three cell phenotypes - CD3+/CD4+ Helper T cells, CD3+/CD8+ Cytotoxic T-cells, and CD3-/CD8+ T-cells (Figure 1A).

We can further classify the Helper T cells using the cell activity biomarkers as inputs for automatic clustering using the PhenoGraph-Leiden method[5,6] on the CD3+/CD4+ phenotype. We have identified four subgroups of CD3+/CD4+ cells (Fig. 1B) – naïve (CD3+/CD4+ only), Regulatory T (Treg) cells (FoxP3+), exhausted T cells (PD-L1+), and actively proliferating cells (Ki67+).

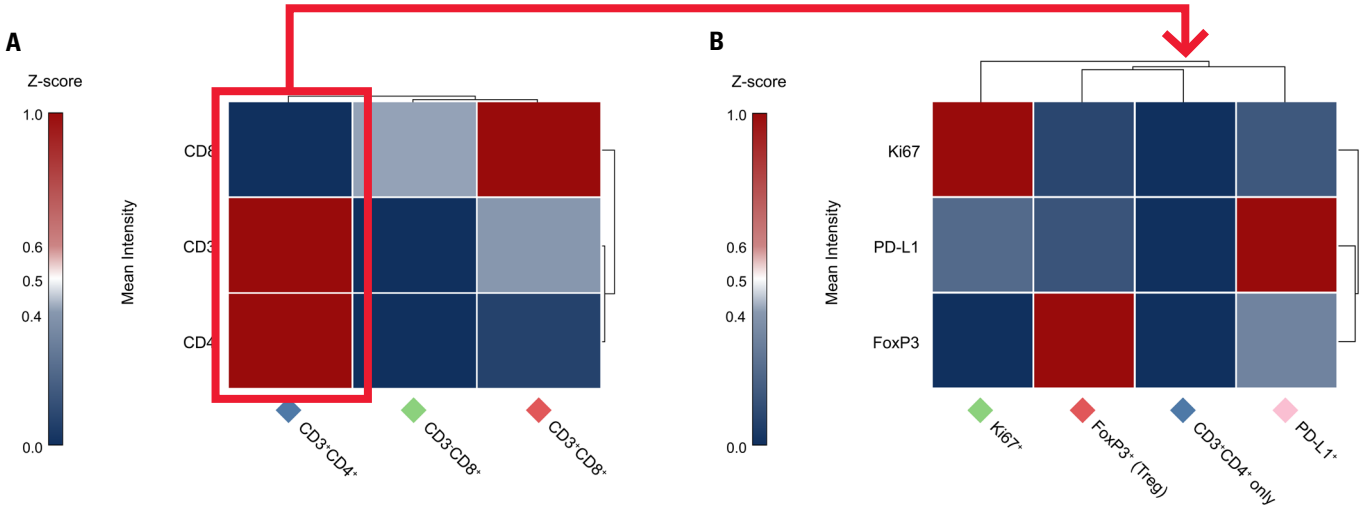

Figure 1. Dendrograms showing the normalized Z-scores for individual biomarker channels for (A) phenotype of all T cells; and (B) subphenotypes of CD3+/CD4+ identified from A.

Spatial analysis of immune and tumor cell proximity

Interaction between immune cell subtypes and tumor cells offers insights into the interplay between the immunity within the tissue and the tumor microenvironment. By analyzing the spatial distributions of immune cell subtypes near cells with a positive tumor marker, we can infer immune activity within the tumor tissue. In Aivia, it is possible to quantify the nearest distance between the immune cells and neighboring tumor cells by looking at their closest, vertex-to-vertex distance. We used the Relation Tool in Aivia to find the nearest five tumor epithelial cells for each T cell and macrophage mapped in the sample. We limited the search range to 20 µm as the typical immune cell-tumor cell effect would only be present within a few microns from the interface. The object relationships are inherited by the cellular phenotypes we have generated in the previous step. Establishing these spatial tumor-to-immune-cell relationships and clusters is the first step for the overall analysis and understanding of the sample.

We found that immune cell sub-phenotypes that are associated with protumor activity from regulatory T cells (FoxP3 positive Treg cells) and from PD-L1 positive activated T cells, are present at their highest concentration within 2 µm of the nearest tumor cells (Figure 2B). This contrasts with the naïve phenotypes of CD3+/CD4+ and CD3+/CD8+, whose highest concentrations are found between 2 and 5 µm away from the tumor cells, with an appreciable amount of them appearing near the tumor cells. The higher presence of Treg cells and reprogrammed T cells, along with naïve T cells near the tumor boundary illustrates the delicate balance between pro- and anti-tumor immune profile that is known to have major drug efficacy relevance in the clinic.

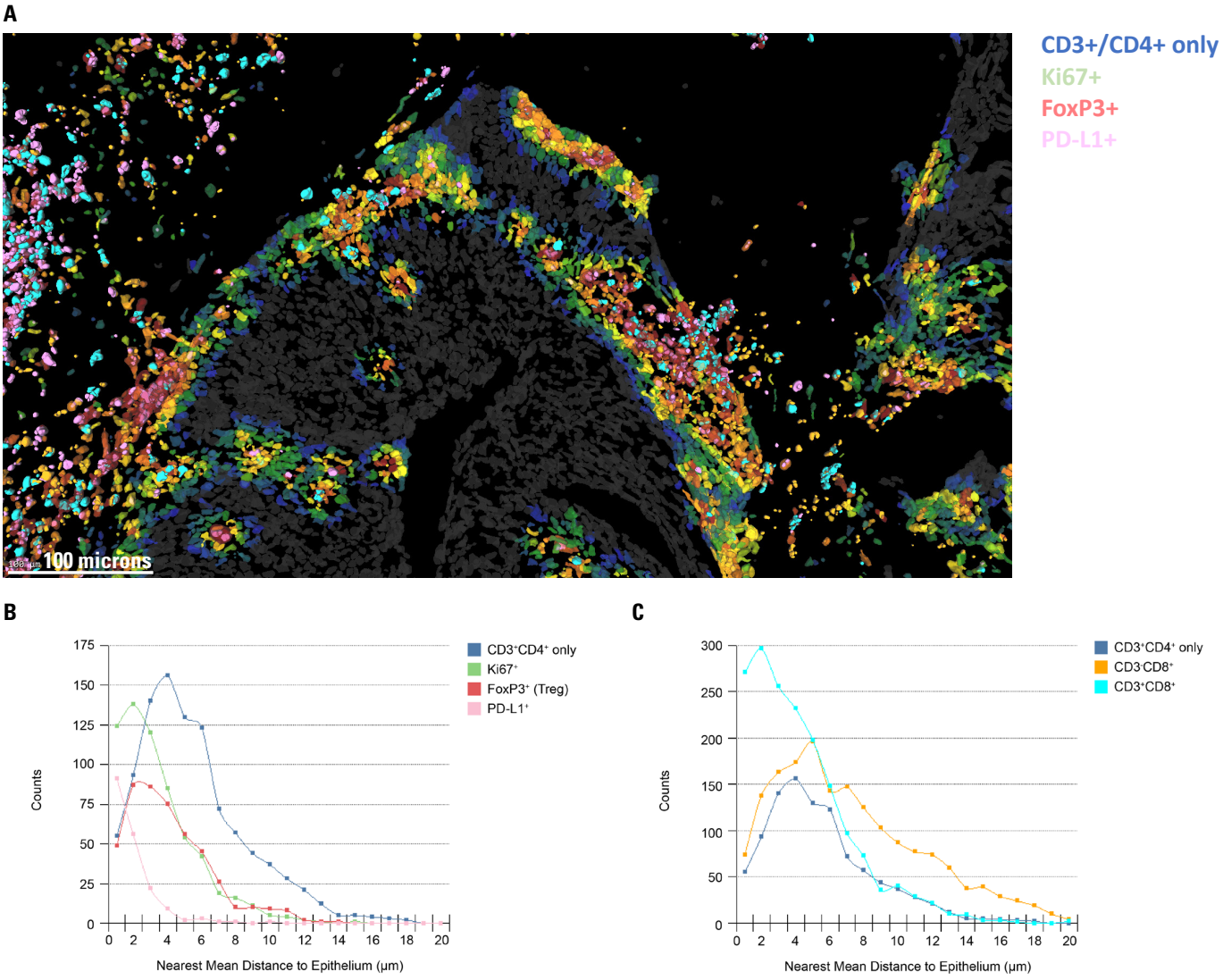

Figure 2. Localization of T cell subphenotypes near epithelial cells. (A) Subphenotypes of CD3+/CD4+ cells with neighboring PanCK+ cells colorized by proximity to the T cells. (B) The subphenotypes of CD3+/CD4+ cells shows different spatial distribution in the mean distance to the nearest five epithelial cells. (C) Spatial distribution of T cells phenotypes (CD3+/CD4+, CD3-/CD8+, CD3+/CD8+) to the nearest five epithelial cells. The CD3+/CD4+ cluster excludes subphenotypes that are coexpressed with one of the state markers (FoxP3, PD-L1, and Ki61).

To investigate the response of the tumor to infiltrating immune cells, we also looked at mean object distance from the tumor epithelial cells to the T cells. At first glance, a plurality of PanCK+ cells are collocated within 2 µm from the nearest immune cell, with a relatively flat distribution of tumor cells between 2 and 12 µm. Plotting the epithelial subphenotypes (Figure 3C) tell a different story, with epithelial cells with high PD-L1 expression showing progressive drop-off in count away from T cells; while both proliferating tumor cells (with Ki67 co-expression) and naïve PanCK+ cells appearing less often in the immediate vicinity of immune cells, peaking at around 8 to 12 µm away (Figure 3D). This illustrates an active front of active immune suppression at the interface, with tumor cell proliferation happening away from immune activities.

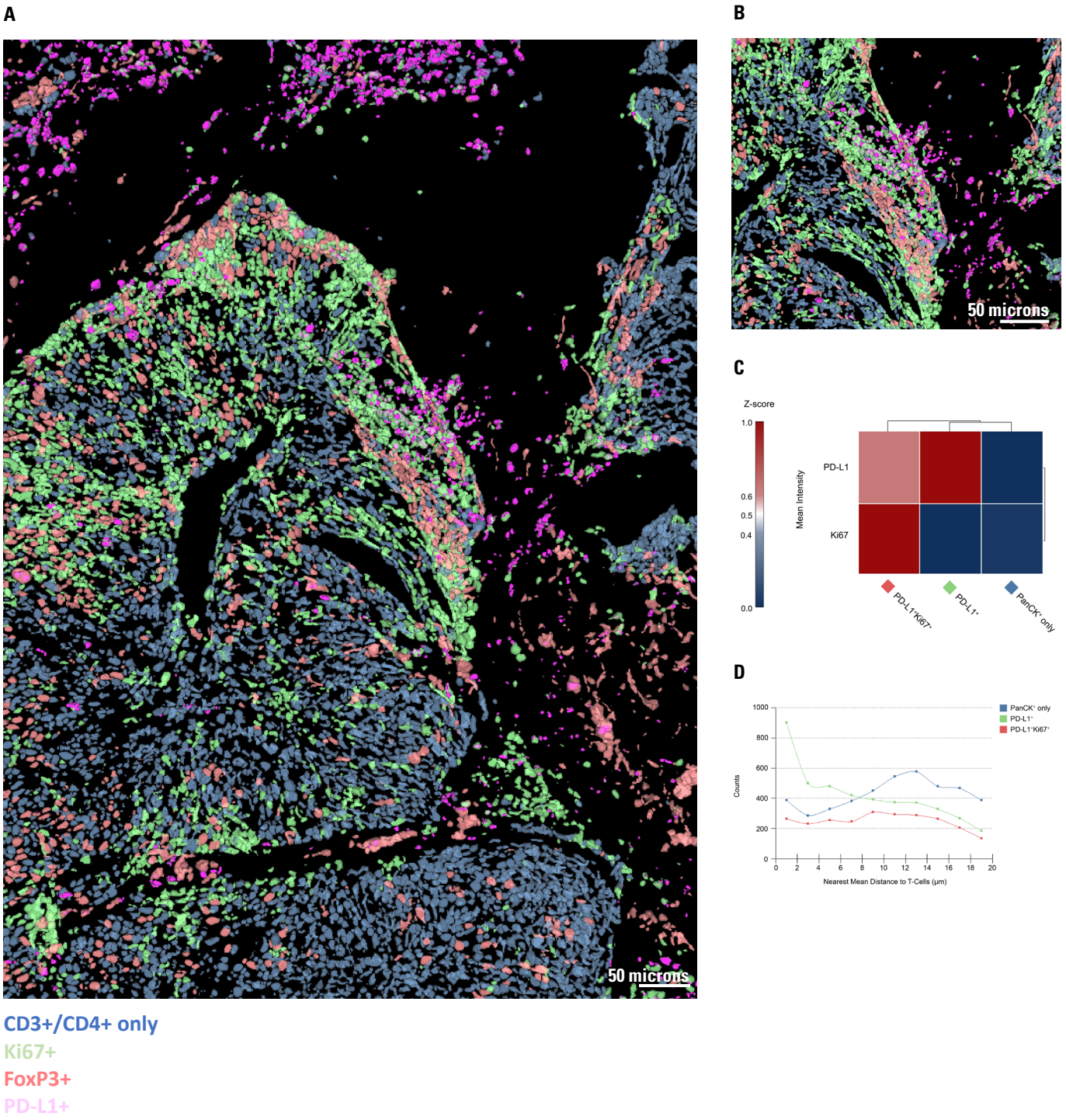

Figure 3. Epithelial cells phenotypes near T cells. (A-B) Segmented lung cancer tissue labeled with a panel of 8 OPAL dyes segmented using the 3D Multiplexed Cell Detection recipe with PanCK+ epithelial cells subclustered using automatic classifier. (C) Dendrogram showing the z-score of PD-L1 and Ki67 channels between the subclusters of PanCK+ cells. Within the lung cancer tissue, (D) PD-L1+ subphenotypes (green) appear to be nearer to the T cells (magenta), compared to the naïve PanCK+ (blue) and proliferating PD-L1+Ki67+ (red) cells.

Discussion

In this experiment, we have leveraged multiplex labeling techniques, 3D confocal imaging, and AI-powered analysis to explore the precise positioning of immune cell populations in proximity to tumor cells. Through this imaging and analysis workflow, we can observe that subtle changes in T cell phenotype and spatial distribution occur in response to tumor activity within the tumor microenvironment. This workflow demonstrates the high granularity of information that can be extracted from tumor microenvironment samples and is made possible by the combination of high-resolution 3D imaging via SpectraPlex and in-depth analysis with Aivia.

While 2D imaging is widely used and conventional in histopathology, the 3D organization of human tissues necessitates 3D imaging approaches for a thorough understanding of cellular morphology and positioning in highly heterogeneous tissues. A useful potential workflow for researchers may be to utilize higher-plex 2D imaging to establish a sub-panel for more in depth and higher resolution 3D confocal imaging. Combining multiplex imaging with Aivia's analysis enables identification of cell phenotypes and analysis of the spatial distribution of the phenotypes within the tissue microenvironment. With the available data, it is possible to infer immune and tumor activities at the interface between immune and tumor cells. A larger, and different, panel of biomarkers would be needed to elucidate the interactions between these cells and their contribution to tumor progression. Nevertheless, a wealth of information can be extracted from these commonly used and widely available dye and label panels.

Aivia enables multiplex analysis of tissue microenvironments in 3D datasets. The combination of 3D imaging and multiplexed cell segmentation and spatial analysis accurately captures the interaction between tumor and immune cells, and much more; and offers unprecedented insights into tumor growth and development.

References

1. de Visser KE, Joyce JA. The evolving tumor microenvironment: From cancer initiation to metastatic outgrowth. Cancer Cell. 2023 Mar 13;41(3):374-403. https://doi.org/10.1016/j.ccell.2023.02.016.

2. Kunz L, Speziale D, Roberti MJ, Susanne, Holzmeister S, Hecht F, Alvarez LAJ, Steinmetz I. 3D high-multiplex imaging in cancer immunology. Nature Methods. 2024. https://www.nature.com/articles/d42473-024-00260-7

3. Roberti, MJ, Hecht F, Gai E, Straka T, Holzmeister S, Steinmetz I, Wong H, Alvarez L SpectraPlex: A powerful toolbox for advanced 3D high-multiplex imaging. Nat. Methods (2024). https://www.nature.com/articles/d42473-024-00262-5.

4. Stringer C, Wang T, Michaelos M, Pachitarius M. Cellpose: a generalist algorithm for cellular segmentation. Nat Methods. 2021; 18, 100–106. https://doi.org/10.1038/s41592-020-01018-x.

5. Levine JH, Simonds EF, Bendall SC, Davis KL, Amir el-AD, Tadmor MD, Litvin O, Fienberg HG, Jager A, Zunder ER, Finck R, Gedman AL, Radtke I, Downing JR, Pe'er D, Nolan GP. Data-Driven Phenotypic Dissection of AML Reveals Progenitor-like Cells that Correlate with Prognosis. Cell. 2015 Jul 2;162(1):184-97. https://doi.org/10.1016/j.cell.2015.05.047.

6. Traag VA, Waltman L, van Eck NJ. From Louvain to Leiden: guaranteeing well-connected communities. Scientific Reports. 2019. 9, 5233. https://doi.org/10.1038/s41598-019-41695-z.

CONNECT
WITH US!

Leica Microsystems CMS GmbH | Ernst-Leitz-Strasse 17–37 | D-35578 Wetzlar (Germany)
Tel. +49 (0) 6441 29-0 | F +49 (0) 6441 29-2599

www.leica-microsystems.com/aivia